

MATFESA: strain and refractive index field estimation after femtosecond laser interaction with transparent material

M. Tejerina · G.A. Torchia

Received: 11 August 2011 / Accepted: 3 August 2012
© Springer-Verlag 2012

Abstract In this paper we present the development of an open code (“MATFESA”) based on the Finite Element Method (FEM) which can be used to estimate the strain and refractive index fields after femtosecond laser writing process by means of an iterative analysis. The fs-laser pulse residual stress control is the key to obtain high performance guiding structures for photonics.

The whole complex physical problem consists in almost three steps inside the material during/after femtosecond laser interaction which cannot be analyzed using thermodynamic equilibrium equations. These are: ionization, expansion and re-solidification.

In the numerical model solved, a mechanical expansion is introduced in the focal plane to simulate laser interaction at intensities above the optical breakdown threshold. Numerical results were compared to experimental measurements of optical guided modes in LiNbO₃ fs-waveguides.

The MATFESA model was compared with ABAQUS commercial software in order to verify the strain field results and also to test the 2D, plane strain approximation.

1 Introduction

In the last decade femtosecond laser writing has emerged as a promising tool for optical circuit fabrication. This fast,

low-cost and easy method can be applied on a large number of materials such as crystals and glasses [1–8]. Several good performance photonic applications generated with this technology have been reported: emitters, lasers, sensors, modulators, etc. [9–12]. In the last years, in order to obtain high performance devices, laser and matter interaction has been deeply studied. Then, it was established that the residual stress field is the main factor responsible for the refractive index increment and light confinement in these kinds of guiding structures. For this reason, from the technological point of view, to control the stress field induced by the laser processing is a necessary mean to improve the waveguide fabrication method. Also, from a basic science point of view, it is important to know how the heated plasma expands and solidifies during ultrafast laser material interaction.

Finite Elements Method (FEM) is well known in physics and engineering sciences. It is used to solve partial differential equations in many subjects: heat transfer, elastic deformation, electrostatic, etc. In this case, the elastic deformation in an anisotropic medium was approximated by using plane strain model and solved by FEM. The code presented in this work was generated using the basic code structure and nomenclature used by Y.W. Kwon [13].

The advantage of generating an open code in MATLAB environment is that this application is massively used in science, so that any user can easily try, use and improve the code for several applications.

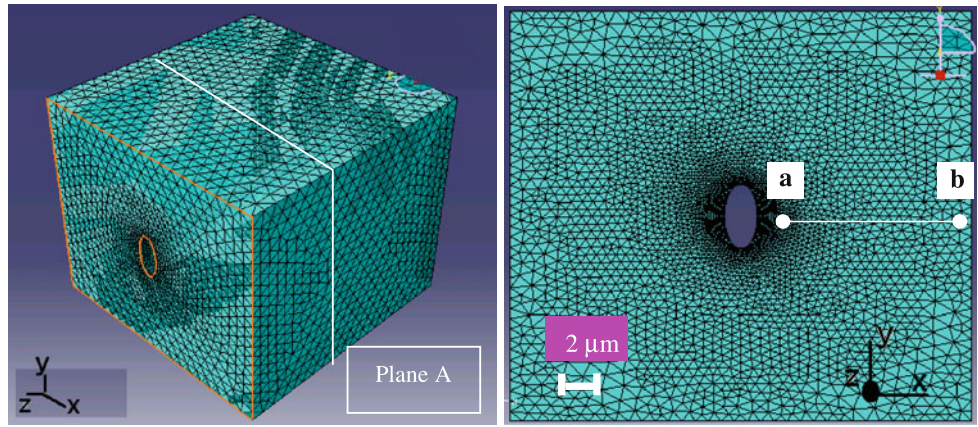
In the Online Resource 1, the parts of the code generated by the authors will be explained in more depth than those not generated by them.

In this work, the problem to be solved by FEM consists in a particular case of an elliptical “hole” which arbitrary expands in an anisotropic elastic infinite medium. A “plane strain” approximation model for anisotropic LiNbO₃ compliance matrix is verified and assumed. Using adequate

Electronic supplementary material The online version of this article (doi:10.1007/s00339-012-7132-y) contains supplementary material, which is available to authorized users.

M. Tejerina · G.A. Torchia (✉)
Centro de Investigaciones Ópticas CONICET La Plata-CIC,
CC n°3 M.B. Gonnert (1897), Pcia. Bs. As., Argentina
e-mail: gustavot@ciop.unlp.edu.ar
Fax: +54-221-4712771

Fig. 1 3D domain (left) and plane strain 2D domain (right)



boundary conditions, two axes of symmetry are also assumed. So the “elliptical hole” geometry is reduced to a quarter of an ellipse. This assumption imparts a limitation in the material compliance matrix symmetry and neglecting of the “shear” refractive index components [14].

In this paper, a possible MATLAB code to be used in this kind of laser and material interaction is presented. Application of this code was implemented to describe fs-laser writing waveguides in LNB crystals.

2 LiNbO₃ orthotropic “plane strain” approximation tested by using abaqus commercial software

A plane strain assumption is used with good results in many works [14, 15]. Before using this assumption, we will discuss when it can be applied to anisotropic material deformations.

Plane strain deformation requires that all deformation not contained in the selected plane be equal to zero. This simplification is applied to isotropic materials and requires that the load not vary in the direction normal to the analyzed plane. For example, it can be used to analyze a cylindrical tube under internal pressure. From a loading and geometric point of view, this example is similar to the problem solved in this work, but from the symmetry of the material point of view, it is not. This is because LiNbO₃ is an anisotropic material, which normally does not allow plane strain deformation [16]. Not all anisotropic materials allow plane strain assumption. Although the load symmetry corresponds to that necessary in plane strain deformation, unless the material plane of symmetry coincides with the selected plane, the plane strain is not allowed (e.g.: if a selected plane is *xz*: $\epsilon_{yy} = 0$ but in general $\epsilon_{zy} \neq 0, \epsilon_{yx} \neq 0$).

For anisotropic materials, if the plane of symmetry coincides with the selected plane, deformation can be decomposed into “in-plane deformations” and “anti-plane deformations”, which are uncoupled deformations [16]. In this

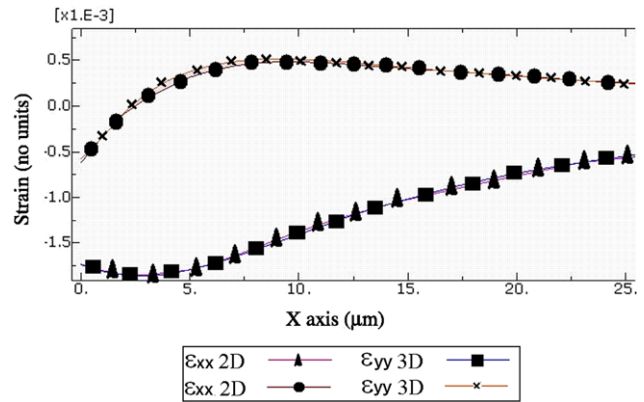


Fig. 2 LiNbO₃ orthotropic approximation compliance matrix (2D) and complete compliance matrix (3D) comparison along path ab

case, plane strain simplification can be used to determine in-plane deformations. A LiNbO₃ crystal does not have a symmetry plane in the analyzed plane (*xz*). It was first time verified in the present work that the plane strain deformation is an acceptable assumption for LiNbO₃ for the material plane (*xz*).

A complete LiNbO₃ compliance matrix in a 3D domain was compared with a LiNbO₃ orthotropic compliance matrix approximation ($C_{14} = 0$) in a plane strain 2D model. Figure 1 depicts a scheme of both domains (2D and 3D). A complete compliance matrix form is given in (1). Analogous boundary conditions and loads (arbitrary internal pressure) were set for both models. The results of this comparison along path *ab* are shown in Fig. 2. They indicate that orthotropic approximation for LiNbO₃ is a valid assumption for the implemented crystal orientation.

$$\begin{bmatrix} S_{xx} \\ S_{yy} \\ S_{zz} \\ S_{xy} \\ S_{xz} \\ S_{yz} \end{bmatrix} = \begin{bmatrix} C_{11} & C_{12} & C_{13} & C_{14} & 0 & 0 \\ : & C_{11} & C_{13} & -C_{14} & 0 & 0 \\ : & : & C_{33} & 0 & 0 & 0 \\ : & : & 0 & C_{44} & 0 & 0 \\ 0 & 0 & 0 & 0 & C_{55} & C_{56} \\ 0 & 0 & 0 & 0 & : & C_{66} \end{bmatrix} \times \begin{bmatrix} \epsilon_{xx} \\ \epsilon_{yy} \\ \epsilon_{zz} \\ \epsilon_{xy} \\ \epsilon_{xz} \\ \epsilon_{yz} \end{bmatrix}, \tag{1}$$

where: “:” means symmetric element,

$$\begin{aligned}
 C_{11} &= 200 \text{ Gpa}, & C_{22} &= 200 \text{ Gpa}, \\
 C_{33} &= 235 \text{ Gpa}, & C_{12} &= 53.3 \text{ Gpa}, \\
 C_{13} &= 67.7 \text{ Gpa}, & C_{14} &= 8.7 \text{ Gpa}, \\
 C_{44} &= 53.5 \text{ Gpa}, & C_{55} &= 53.5 \text{ Gpa}, \\
 C_{66} &= 53.5 \text{ Gpa}, & C_{56} &= 9.7 \text{ Gpa}, \\
 S_{ij} &= ij \text{ component of stress,} \\
 \varepsilon_{ij} &= ij \text{ component of strain tensor.}
 \end{aligned}$$

3 Results: displacement estimation with MATFESA code and experimental comparison

3.1 Displacement estimation

Information about the mesh generation and boundary conditions’ application is given in Online Resource 1. Also, in this document, a strain field obtained with MATFESA is compared to that obtained with ABAQUS to verify the generated

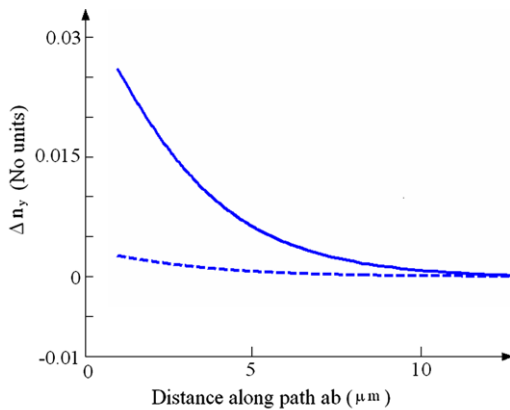
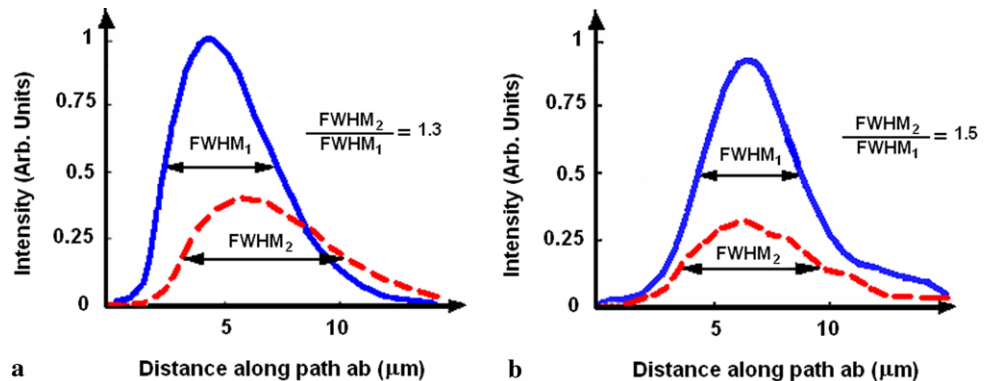


Fig. 3 Refractive index variation along path ‘ab’ estimated with MATFESA. The *solid line* represents a 12 % of area variation ($\Delta V/V = 0.12$) and the *dashed line* represents a 1.2 % of area variation ($\Delta V/V = 0.012$)

Fig. 4 (a) Theoretical intensity profile comparison between optical modes guided using $\Delta V/V_1 = 0.12$ (*solid line*) and $\Delta V/V_2 = 0.012$ (*dashed line*). (b) Experimental comparison of guided mode between fs-waveguide 1 ($v = 0.1$ mm/s) and fs-waveguide 2 ($v = 0.02$ mm/s)



code. This was carried out using the same boundary conditions in both models and they gave consistent results.

Once the mesh, the boundary conditions and the material properties are set, the code follows the same structure used in [13] to estimate the *disp* vector. The *disp* is a vector containing displacement solutions for each node in x and y directions.

3.2 Experimental comparison

To show one of the possible applications of the generated code, we estimated the refractive index field along path ‘ab’ (see Fig. 1) for two different volume expansions ($\Delta V/V_1 = 12\%$ and $\Delta V/V_2 = 1.2\%$) of the central ellipse, as is shown in Fig. 3. Then, using R-Soft commercial software, we estimated the intensity profile assuming a plane waveguide with mentioned refractive index variations (Δn_1 and Δn_2) along path ‘ab’. A comparison of resulting intensity profiles is shown in Fig. 4(a); as can be seen, the Full Widths at Half Maximum (FWHMs) of the two profiles are different, being wider for the profile corresponding to the minimum expansion ($\Delta V/V_1$). The ratio $\Gamma = \text{FWHM}_2/\text{FWHM}_1$ is about 1.3.

According to the existing literature [17], to increase expansion in the fs-laser process, fs-waveguides can be generated with different writing speeds. Taking into account this, we generated two different waveguides with processing velocities of 0.1 mm/s (fs-waveguide 1) and 0.02 mm/s (fs-waveguide 2). The energy per pulse was set to 3 μJ , the repetition rate was 100 KHz and a 20x microscope objective was used for focusing. The propagated guided modes at 532 nm from these waveguides were registered by using a CCD intensity beam profiler. These guided modes profiles along path ‘ab’ were compared as is shown in Fig. 4(b). As it can be seen, they show different FWHMs, obtaining $\Gamma = 1.5$.

Comparing parts (a) and (b) of Fig. 4 and taking into account the similar values of Γ obtained in experimental and theoretical results, it can be concluded that the guided mode FWHM behavior for different writing speeds by using different expansions $\Delta V/V$ can be modeled with MATFESA code.

4 Conclusions

A MATLAB code was developed to estimate refractive index field after femtosecond laser interaction with transparent materials.

The assumption of “plane strain” used in this work and by other authors [14, 15] for LiNbO₃ was verified with a 3D ABAQUS model. Besides, the MATFESA model strain result was compared with a plane strain ABAQUS model strain result. Good accordance is reached between them.

Finally, the refractive index field obtained using MATFESA is in good accordance with that described in the existing literature [14, 15].

Also, a comparison of experimental results of fs-waveguide intensity mode profile and theoretical predictions was carried out. These waveguides were generated using different processing conditions. In this analysis, it was concluded that the guided mode FWHM behavior for different writing speeds can be modeled with MATFESA code with good results. This behavior is given by increasing the FWHM for the guided modes when there is an increase of the writing speed.

We conclude that the open code for MATLAB environment, MATFESA, is an adequate means for iterative analysis of femtosecond laser written waveguides generated in crystals with appropriate symmetry or isotropic materials.

The advantage of this open code in MATLAB environment is that it can be easily used and improved for scientific and technical applications.

Acknowledgements The authors wish to thank CONICET and Agencia Nacional de Promoción Científica y Tecnológica (Argentina) for financial support received for this work under projects PIP 0394 and PICT 2575.

Note MATFESA code can be freely received by sending an email to the following addresses: gustavot@ciop.unlp.edu.ar, matiast@ciop.unlp.edu.ar.

References

1. K. Miura, J. Qui, H. Inouye, T. Mitsuyu, K. Hirao, *Appl. Phys. Lett.* **71**, 3329–3331 (1997)
2. A.M. Strelsov, N.F. Borrelli, *J. Opt. Soc. Am. B* **19**, 2496–2504 (2002)
3. M. Will, S. Nolte, B.N. Chichkov, A. Tunnermann, *Appl. Opt.* **41**, 4360–4364 (2002)
4. C. Florea, K.A. Winick, Fabrication and characterization of photonic devices directly written in glass using femtosecond laser pulses. *J. Lightwave Technol.* **21**, 246–253 (2003)
5. S. Taccheo, G. Della Valle, R. Osellame, G. Cerullo, N. Chiodo, P. Laporta, O. Svelto, A. Killi, U. Morgner, M. Lederer, D. Kopf, *Opt. Lett.* **29**, 1900–1902 (2004)
6. C. Méndez, J.R. Vázquez de Aldana, G.A. Torchia, L. Roso, *Appl. Phys. B, Laser Opt.* **86**, 243 (2007)
7. A. Ródenas, L.M. Maestro, M.O. Ramírez, G.A. Torchia, L. Roso, F. Chen, D. Jaque, Anisotropic lattice changes in femtosecond laser inscribed Nd³⁺:MgO:LiNbO₃ optical waveguides. *J. Appl. Phys.* **106**, 013110-6 (2009)
8. G. De Lavallo, R. Osellame, P. Laporta, Micromachining of photonic devices by femtosecond laser pulses. *J. Opt. A, Pure Appl. Opt.* **11**, 013001 (2009)
9. G.A. Torchia, A. Ródenas, A. Benayas, L. Roso, D. Jaque, Highly efficient laser action in femtosecond-written Nd:yttrium aluminum crystals. *Appl. Phys. Lett.* **92**, 111103 (2008)
10. C. Vannahme, H. Suche, S. Reza, R. Ricken, V. Quiring, W. Sohler, Integrated optical Ti:LiNbO₃ ring resonator for rotation rate sensing, in *Proceedings of European Conference on Integrated Optics* (2007)
11. M.R. Tejerina, G.A. Torchia, *Appl. Opt.* **50**(20), 3449–3454 (2011)
12. S. Ringleb, K. Rademaker, S. Nolte, A. Tünnermann, Monolithically integrated optical frequency converter and amplitude modulator in LiNbO₃ fabricated by femtosecond laser pulses. *Appl. Phys. B* **102**, 59–63 (2011)
13. Y.W. Kwon, H. Bang, *Finite Element Method Using MATLAB* (1997)
14. J. Burghoff, S. Nolte, A. Tünnermann, *Appl. Phys. A* **89**(1), 127 (2007)
15. M. Will, J. Burghoff, S. Nolte, A. Tünnermann, Detailed investigations on femtosecond induced modifications in crystalline quartz for integrated optical applications, in *Conference “Commercial and Biomedical Applications of Ultrafast Lasers”* (2005)
16. T.C. Ting, *Anisotropic Elasticity: Theory and Applications* (Oxford University Press, London, 1996)
17. C.B. Schaffer, Interaction of femtosecond laser pulses with transparent materials, Thesis, 2001